

1 **[Technical note] 3-hourly temporal downscaling of monthly global**  
2 **terrestrial biosphere model net ecosystem exchange**

3

4 Joshua B. Fisher<sup>1,\*</sup>, Munish Sikka<sup>1</sup>, Deborah N. Huntzinger<sup>2</sup>, Christopher  
5 Schwalm<sup>3</sup>, Junjie Liu<sup>1</sup>

6

7 <sup>1</sup> Jet Propulsion Laboratory, California Institute of Technology, 4800 Oak Grove Drive, Pasadena, CA, 91109, USA

8 <sup>2</sup> School of Earth Sciences and Environmental Sustainability, Northern Arizona University, 527 S. Beaver St.,  
9 Flagstaff, AZ, 86011-5694, USA

10 <sup>3</sup> Woods Hole Research Center, Falmouth, MA, 02540, USA

11 \* *Corresponding author. E-mail: jbfisher@jpl.nasa.gov*

12

13 Author contributions: JBF, DNH, and CS formulated idea; JBF and MS designed research; MS performed research;  
14 DNH and CS provided data; all authors contributed to the writing of the paper.

15

16 The authors declare no conflict of interest.

17

18 Running title: 3-hourly temporal downscaling of monthly NEE

19 **Abstract**

20 The land surface provides a boundary condition to atmospheric forward and flux inversion  
21 models. These models require prior estimates of CO<sub>2</sub> fluxes at relatively high temporal  
22 resolutions (e.g., 3-hourly) because of the high frequency of atmospheric mixing and wind  
23 heterogeneity. However, land surface model CO<sub>2</sub> fluxes are often provided at monthly time steps,  
24 typically because the land surface modeling community focuses more on time steps associated  
25 with plant phenology (e.g., seasonal) than on sub-daily phenomena. Here, we describe a new  
26 dataset created from 15 global land surface models and 4 ensemble products in the Multi-scale  
27 Synthesis and Terrestrial Model Intercomparison Project (MsTMIP), temporally downscaled  
28 from monthly to 3-hourly output. We provide 3-hourly output for each individual model over 7  
29 years (2004-2010), as well as an ensemble mean, a weighted ensemble mean, and the multi-  
30 model standard deviation. Output is provided in three different spatial resolutions for user  
31 preferences: 0.5° x 0.5°, 2.0° x 2.5°, and 4.0° x 5.0° (latitude/longitude). These data are publicly  
32 available from: [ftp://daac.ornl.gov/data/cms/CMS\\_NEE\\_CO2\\_Fluxes\\_TBMO/data](ftp://daac.ornl.gov/data/cms/CMS_NEE_CO2_Fluxes_TBMO/data).

33  
34 *Keywords: CO<sub>2</sub> flux; downscale; land surface; NEE; sub-daily; hourly*

35 This technical note describes the methodological approach employed with temporally  
 36 downscaling monthly terrestrial biosphere model (TBM) net ecosystem exchange (*NEE*) (i.e., net  
 37 CO<sub>2</sub> flux between the land and atmosphere) output to 3-hourly time steps (Fisher et al., 2014).  
 38 These data were created initially for NASA's Carbon Monitoring System (CMS), and are useful  
 39 to the broader land surface and atmospheric scientific community (Fisher et al., 2011; Fisher et  
 40 al., 2012). The general downscaling approach follows Olsen and Randerson (2004) with  
 41 modifications. The logic takes the components of *NEE*, i.e., gross primary production (*GPP*) and  
 42 ecosystem respiration (*Re*), and links them with incident shortwave solar radiation (*I*) and near  
 43 surface (2 m) air temperature (*T<sub>a</sub>*), respectively. *I* and *T<sub>a</sub>* are provided at 6-hourly time steps from  
 44 CRU-NCEP (Wei et al., 2014a; Wei et al., 2014b), which we interpolated to 3-hourly time steps  
 45 following cosines of solar zenith angle for *I* and linear interpolation for *T<sub>a</sub>*. Hence, *GPP* and *Re*  
 46 are temporally downscaled to 3-hourly, and re-combined to form *NEE* at 3-hourly time steps.

47  
 48 The 6-hourly to two 3-hourly time steps from the solar zenith angle cosine interpolation follows  
 49 this equation:

$$I_{t1} = \frac{I_t \times \cos z_{t1}}{\left(\frac{\cos z_{t1} + \cos z_{t-t1}}{2}\right)}, I_{t-t1} = \frac{I_t \times \cos z_{t-t1}}{\left(\frac{\cos z_{t1} + \cos z_{t-t1}}{2}\right)} \quad (1)$$

50 where *z* is solar zenith angle and *I<sub>t</sub>* is in units of W m<sup>-2</sup>. As an example, if the 0-6 hour *I<sub>t</sub>* was 100  
 51 W m<sup>-2</sup>, and the 0-3 hour *z<sub>t1</sub>* was 0 (i.e., cos(*z<sub>t1</sub>*) = 1) and the 4-6 hour *z<sub>t-t1</sub>* was 60 (i.e., cos(*z<sub>t-t1</sub>*) =  
 52 0.5), then the 0-3 hour *I<sub>t1</sub>* would be 133.3 W m<sup>-2</sup>, and the 4-6 hour *I<sub>t-t1</sub>* would be 66.7 W m<sup>-2</sup>.

53  
 54 To scale *GPP* and *Re* to 3-hourly time steps, we followed Olsen and Randerson (2004) with  
 55 modifications starting first with the calculation of scale factors based on *I* and *T<sub>a</sub>*:

$$Q10_{3hr} = 1.5^{\frac{T_{a,3hr} - 30}{10}} \quad (2a)$$

$$T_{scale} = Q10_{3hr} / \sum_{30day} Q10_{3hr} \quad (2b)$$

$$I_{scale} = I_{3hr} / \sum_{30day} I_{3hr} \quad (3)$$

56 where *Q10* is the temperature dependency of *Re*, and *T<sub>a</sub>* is in degrees Celsius (converted from  
 57 Kelvin, as provided by CRU-NCEP). Note that Olsen and Randerson (2004) originally used time  
 58 integral periods of calendar months, but we observed that this caused unrealistic distinct shifts  
 59 between months. Instead, we modified the integral period to a 30-day moving window (Figure 1).  
 60 For the first 15 days of January of the record and the last 15 days of December of the record, we  
 61 used the last 15 days of December and the first 15 days of January, respectively, within the first  
 62 (2004) and last (2010) years to complete the 30-day window.

63  
 64 The 3-hourly resolution scale factors are then multiplied by *GPP* and *Re*, respectively, for each  
 65 3-hourly time step each month:

$$Re_{3hr} = T_{scale} \times Re_{month} \quad (4)$$

$$GPP_{3hr} = I_{scale} \times GPP_{month} \quad (5)$$

66 We modified *Re<sub>month</sub>* and *GPP<sub>month</sub>* from Olsen and Randerson (2004) to be given at a 3-hourly  
 67 time step, linearly interpolated to 3-hourly time steps based on the present, previous, and  
 68 subsequent month, maintaining the original units (g C m<sup>-2</sup> mo<sup>-1</sup>). *Re<sub>3hr</sub>* and *GPP<sub>3hr</sub>* are in units of  
 69 g C m<sup>-2</sup> 3hr<sup>-1</sup>. This modification avoided using the same monthly value for the multiplier for all  
 70 3-hourly time steps per month as per Olsen and Randerson (2004), and instead provided a

71 smooth transition from one month to the next. The result of this modification was to eliminate a  
72 “ramping” effect whereby values would, for example, increase steadily within a month, then  
73 suddenly shift to a new starting point at the beginning of the next month (Figure 1). Note that the  
74 original nomenclature of Olsen and Randerson (2004) used  $[(2 \times NPP_{month}) - NEP_{month}]$  in  
75 place of  $Re_{month}$ , and  $(2 \times NPP_{month})$  in place of  $GPP_{month}$ , where  $NPP$  is net primary production  
76 ( $GPP$  minus autotrophic respiration) and  $NEP$  is net ecosystem production (approximately  
77 equivalent to the inverse sign of  $NEE$ , with caveats (Hayes and Turner, 2012)). The assumption  
78 here, therefore, is that  $GPP = 2 \times NPP$  and  $Re = (2 \times NPP) - NEP$ . The  $Re$  assumption misses  
79  $CO_2$  emissions other than respiration, e.g., fire, which we correct for at a later step.

80  
81 The initial  $NEE$  calculation simply subtracts  $GPP$  from  $Re$ :

$$NEE_{3hr} = Re_{3hr} - GPP_{3hr} \quad (4)$$

82 where  $NEE_{3hr}$  is calculated in units of  $g\ C\ m^{-2}\ 3hr^{-1}$ . However, we applied an additional units  
83 conversion for the publicly available data to  $kg\ C\ km^{-2}\ s^{-1}$ , as these units are more readily  
84 ingestible by atmospheric inversion models (Deng et al., 2014).

85  
86 Because the downscaling approach uses  $Re$  (e.g., autotrophic plus heterotrophic respiration) as  
87 the primary  $CO_2$  efflux term, other ecosystem  $CO_2$  loss components, such as fire and other  
88 disturbances (Hayes and Turner, 2012), are excluded in the downscale. Hence, the sum of the  
89 downscaled 3-hourly  $NEE$  fluxes in a given month did not necessarily equal the original monthly  
90  $NEE$  flux. So, we included a per-pixel correction whereby we: I) calculated the difference  
91 between the sum of the downscaled 3-hourly  $NEE$  in a given month and the original monthly  
92  $NEE$ ; II) divided that difference by the total 3-hourly time steps in the month, and III) added that  
93 difference to each 3-hourly  $NEE$  flux. In so doing, the sum of the downscaled 3-hourly  $NEE$   
94 fluxes subsequently summed exactly to the original monthly  $NEE$ . Nonetheless, this assumption  
95 smooths what could otherwise be punctuated fire or disturbance effluxes, so caution should be  
96 given when assessing these effluxes at 3-hourly time steps (e.g., relative to observations).

97  
98 All input data were given in a spatial resolution of  $0.5^\circ \times 0.5^\circ$  (latitude/longitude); hence, we  
99 provide the 3-hourly  $NEE$  output in  $0.5^\circ \times 0.5^\circ$  (Figure 2). We also provide two additional sets of  
100 spatially upscaled  $NEE$  output in  $2.0^\circ \times 2.5^\circ$  and  $4.0^\circ \times 5.0^\circ$ . These resolutions are used by the  
101 atmospheric modeling community, i.e., the GEOS-Chem atmospheric  $CO_2$  transport model in the  
102 NASA CMS (Liu et al., 2014). To generate the coarser resolution data we: I) multiplied each  
103 pixel value by the land area of that pixel; II) summed the flux from all pixels that represent one  
104 pixel in coarser resolution (e.g.,  $8 \times 10$  pixels from  $0.5^\circ \times 0.5^\circ$  comprise 1 pixel in  $4.0^\circ \times 5.0^\circ$ );  
105 III) calculated the total area covered by the pixels summed in step II; and, IV) divided the value  
106 in step II by the value in step III. The regridding preserved the total sum flux of the finer grid  
107 cells as well as the total global flux. We provide a file containing the land area contained in each  
108 latitudinal band for each of the 3 resolutions (folder name: ‘latitude\_area’). We provide two  
109 versions of the  $2.0^\circ \times 2.5^\circ$  and  $4.0^\circ \times 5.0^\circ$  resolution products—one version with consistent  
110 global resolution, and another that conforms to the GEOS-Chem setup whereby the northern and  
111 southern most latitudinal bands for the  $2.0^\circ \times 2.5^\circ$  resolution are  $1.0^\circ \times 2.5^\circ$ , and for the  $4.0^\circ \times$   
112  $5.0^\circ$  they are  $2.0^\circ \times 5.0^\circ$ . The orientation of the global grid in the NetCDF files is transposed (i.e.,  
113  $90^\circ S \times 180^\circ W$  at top-left). The time vector represents the mid-point of each 3-hourly period.

115 Processing time in R, un-parallelized, on a standard PC for a single year for the forcing data was  
116 as follows:

- 117 • Interpolation of 6-hourly  $I$  and  $T_a$  to 3-hourly time step: 1 hr per variable
- 118 • 30-day moving window for  $I$ : 48 hr
- 119 • 30-day moving window for  $T_a$ : 68 hr
- 120 • *Total time to process forcing data for 7 years:  $7*(1*2+48+68) = 826$  hr*

121  
122 Processing time for the application of the modified Olsen and Randerson (2004) downscaling  
123 approach for a single model for a single year was:

- 124 • Monthly interpolation to 3-hourly time steps for  $GPP$ : 1 hr
- 125 • Monthly interpolation to 3-hourly time steps for  $Re$ : 1 hr
- 126 •  $GPP$  and  $Re$  downscaling: 2 hr
- 127 • Monthly  $NEE$  closure correction: 1 hr
- 128 • NetCDF generation with additional spatial resolutions: 2 hr
- 129 • *Total time to process all 19 products for 7 years:  $7*19*(1+1+2+1+2) = 931$  hr*

130  
131 The total storage size of the final NetCDF data products for all 19 products (15 models + 4  
132 ensemble products) for all 7 years is: 374 GB at  $0.5^\circ \times 0.5^\circ$ , 38 GB at  $2.0^\circ \times 2.5^\circ$ , and 10 GB at  
133  $4.0^\circ \times 5.0^\circ$ .

134  
135 We provide the data in NetCDF with a separate file for each day per product at  
136 [ftp://daac.ornl.gov/data/cms/CMS\\_NEE\\_CO2\\_Fluxes\\_TBMO/data](ftp://daac.ornl.gov/data/cms/CMS_NEE_CO2_Fluxes_TBMO/data) (Fisher et al., 2016). Each  
137 file contains the global gridded data with the eight 3-hourly intervals in the day. Open water  
138 pixels are set to 0, as this was desired by the atmospheric modeling community. However, we  
139 realize that  $NEE$  values can conceivably be 0 (though unlikely as our precision is to 16 decimal  
140 places); nonetheless, there are some pixels over land that are calculated as 0, but this is due to  
141 missing forcing data (e.g.,  $I$  in the high latitudes during winter). Our code is set up that we can  
142 easily provide a different file output structure and missing value mask by request (contact the  
143 corresponding author: [jbfisher@jpl.nasa.gov](mailto:jbfisher@jpl.nasa.gov)).

144  
145 Model output ( $GPP$ ,  $Re$ , and  $NEE$ ) was from the Multi-scale Synthesis and Terrestrial Model  
146 Intercomparison Project (MsTMIP) (Huntzinger et al., 2013; Huntzinger et al., 2016), version 1.  
147 15 models were included: 1) BIOME\_BGC, 2) CLM, 3) CLM4VIC, 4) CLASS\_CTEM, 5)  
148 DLEM, 6) GTEC, 7) ISAM, 8) LPJ-wsl, 9) ORCHIDEE, 10) SIB3, 11) SIBCASA, 12) TEM6,  
149 13) TRIPLEX-GHG, 14) VEGAS2.1, and 15) VISIT (Table 1). All models were driven by CRU-  
150 NCEP meteorological forcing data, hence our use of the same data source for the downscaling  
151 approach applied here. We note that there are other meteorological forcing datasets also available  
152 at 3-hourly time steps for those interested in applying our downscaling approach with different  
153 data (Sheffield et al., 2006; Weedon et al., 2011; Weedon et al., 2014). Although some models  
154 are capable of output at sub-monthly time steps, the standard MsTMIP output is at the monthly  
155 time step. Additionally, 4 ensemble products were included: 1) un-weighted (naïve) ensemble  
156 mean, 2) un-weighted (naïve) ensemble standard deviation, 3) weighted (optimal) ensemble  
157 mean, and 4) weighted (optimal) ensemble standard deviation. Weights for model ensemble  
158 integration were derived based on model skill in reproducing  $GPP$  and biomass (Schwalm et al.,  
159 2015). Model output was obtained from:  
160 <ftp://nacp.ornl.gov/synthesis/2009/reutlingen/CMS/20141006/>

161  
162 To test and confirm that our downscaling approach was applied correctly, we tested our method  
163 on a set of ground-truth data of measured *NEE* (and forcing variables) from the FLUXNET  
164 database (Baldocchi et al., 2001). We show, for example, a single year for a single site (3-hourly  
165 in background with daily-moving window overlaid) (Figure 3) and the scatterplot of calculated  
166 versus observed *NEE* values at the 3-hourly time step for that site and year (Figure 4). A full  
167 uncertainty analysis of the approach is beyond the scope of this technical note intended to  
168 describe the methodological detail of the downscaling.

169 **Acknowledgements**

170 Funding for this work was provided by NASA’s Carbon Monitoring System (CMS) and NASA’s  
171 Carbon Cycle Science (CARBON) programs. We thank the MsTMIP modeling teams for  
172 providing the model output. Access and information about MsTMIP model output can be found  
173 at <http://nacp.ornl.gov/mstmipdata/>, along with model and model team participant information.  
174 Funding for the MsTMIP activity was provided through NASA ROSES Grant  
175 #NNX10AGO01A. Data management support for preparing, documenting, and distributing  
176 MsTMIP model driver and output data was performed by the Modeling and Synthesis Thematic  
177 Data Center at Oak Ridge National Laboratory with funding through NASA ROSES Grant  
178 #NNH10AN681. We thank Dennis Baldocchi and Siyan Ma for providing the Tonzi Ranch  
179 AmeriFlux/FLUXNET data; funding for AmeriFlux data resources and core site data was  
180 provided by the U.S. Department of Energy’s Office of Science. Two reviewers provided useful  
181 suggestions to improving the paper. The research was carried out at the Jet Propulsion  
182 Laboratory, California Institute of Technology, under a contract with the National Aeronautics  
183 and Space Administration. Government sponsorship acknowledged. Copyright 2016. All rights  
184 reserved.

185 **References**

- 186 Baker, I. T., Prihodko, L., Denning, A. S., Goulden, M., Miller, S., and da Rocha, H. R.:  
187 Seasonal drought stress in the Amazon: Reconciling models and observations, *J. Geophys. Res.*,  
188 113, G00B01, 2008.
- 189
- 190 Baldocchi, D., Falge, E., Gu, L. H., Olson, R. J., Hollinger, D., Running, S. W., Anthoni, P. M.,  
191 Bernhofer, C., Davis, K., Evans, R., Fuentes, J., Goldstein, A., Katul, G., Law, B. E., Lee, X. H.,  
192 Malhi, Y., Meyers, T., Munger, W., Oechel, W., U, K. T. P., Pilegaard, K., Schmid, H. P.,  
193 Valentini, R., Verma, S., Vesala, T., Wilson, K., and Wofsy, S. C.: FLUXNET: A new tool to  
194 study the temporal and spatial variability of ecosystem-scale carbon dioxide, water vapor, and  
195 energy flux densities, *Bulletin of the American Meteorological Society*, 82, 2415-2434, 2001.
- 196
- 197 Baldocchi, D. and Ma, S.: How will land use affect air temperature in the surface boundary  
198 layer? Lessons learned from a comparative study on the energy balance of an oak savanna and  
199 annual grassland in California, USA, *Tellus B*, 65, 2013.
- 200
- 201 Deng, F., Jones, D., Henze, D., Bousserez, N., Bowman, K., Fisher, J., Nassar, R., O'Dell, C.,  
202 Wunch, D., and Wennberg, P.: Inferring regional sources and sinks of atmospheric CO<sub>2</sub> from  
203 GOSAT XCO<sub>2</sub> data, *Atmospheric Chemistry and Physics*, 14, 3703-3727, 2014.
- 204
- 205 Fisher, J. B., Huntzinger, D. N., Schwalm, C. R., and Sitch, S.: Modeling the terrestrial biosphere,  
206 *Annual Review of Environment and Resources*, 39, 91-123, 2014.
- 207
- 208 Fisher, J. B., Polhamus, A., Bowman, K. W., Liu, J., Lee, M., Jung, M., Reichstein, M., Collatz,  
209 G. J., and Potter, C.: Evaluation of NASA's Carbon Monitoring System Flux Pilot: terrestrial  
210 CO<sub>2</sub> fluxes, San Francisco, CA2011.
- 211
- 212 Fisher, J. B., Sikka, M., Bowman, K. W., Liu, J., Lee, M., Collatz, G. J., Pawson, S., Gunson, M.,  
213 CMS Flux Team, TRENDY Modelers, and NACP Regional Synthesis Modelers: The NASA  
214 Carbon Monitoring System (CMS) Flux Pilot Project as a means to evaluate global land surface  
215 models, American Geophysical Union Fall Meeting, San Francisco, 2012.
- 216
- 217 Fisher, J. B., Sikka, M., Huntzinger, D. N., Schwalm, C. R., Liu, J., Wei, Y., Cook, R. B.,  
218 Michalak, A. M., Schaefer, K., Jacobson, A. R., Arain, M. A., Ciais, P., El-Masri, B., Hayes, D.  
219 J., Huang, M., Huang, S., Ito, A., Jain, A. K., Lei, H., Lu, C., Maignan, F., Mao, J., Parazoo, N.,  
220 Peng, C., Peng, S., Poulter, B., Ricciuto, D. M., Tian, H., Shi, X., Wang, W., Zeng, N., Zhao, F.,  
221 and Zhu, Q.: CMS: Modeled Net Ecosystem Exchange at 3-hourly Time Steps, 2004-2010.  
222 ORNL DAAC, Oak Ridge, Tennessee, USA, 2016.
- 223
- 224 Hayes, D. and Turner, D.: The need for “apples - to - apples” comparisons of carbon dioxide  
225 source and sink estimates, *Eos, Transactions American Geophysical Union*, 93, 404-405, 2012.
- 226
- 227 Hayes, D. J., McGuire, A. D., Kicklighter, D. W., Gurney, K. R., Burnside, T. J., and Melillo, J.  
228 M.: Is the northern high-latitude land-based CO<sub>2</sub> sink weakening?, *Global Biogeochemical*  
229 *Cycles*, 25, 2011.
- 230



231 Huang, S., Arain, M. A., Arora, V. K., Yuan, F., Brodeur, J., and Peichl, M.: Analysis of  
232 nitrogen controls on carbon and water exchanges in a conifer forest using the CLASS-CTEM N+  
233 model, *Ecological Modelling*, 222, 3743-3760, 2011.

234

235 Huntzinger, D., Schwalm, C., Michalak, A., Schaefer, K., King, A., Wei, Y., Jacobson, A., Liu,  
236 S., Cook, R., Post, W., Berthier, G., Hayes, D., Huang, M., Ito, A., Lei, H., Lu, C., Mao, J., Peng,  
237 C., Peng, S., Poulter, B., Ricciuto, D., Shi, X., Tian, H., Wang, W., Zeng, N., Zhao, F., and Zhu,  
238 Q.: The North American Carbon Program Multi-scale synthesis and Terrestrial Model  
239 Intercomparison Project–Part 1: Overview and experimental design, *Geoscientific Model  
240 Development*, 6, 2121-2133, 2013.

241

242 Huntzinger, D. N., Schwalm, C. R., Wei, Y., Cook, R. B., Michalak, A. M., Schaefer, K.,  
243 Jacobson, A. R., Arain, M. A., Ciais, P., Fisher, J. B., Hayes, D. J., Huang, M., Huang, S., Ito, A.,  
244 Jain, A. K., Lei, H., Lu, C., Maignan, F., Mao, J., Parazoo, N., Peng, C., Peng, S., Poulter, B.,  
245 Ricciuto, D. M., Tian, H., Shi, X., Wang, W., Zeng, N., Zhao, F., and Zhu, Q.: NACP MsTMIP:  
246 Global 0.5-deg Terrestrial Biosphere Model Outputs (version 1) in Standard Format. DAAC, O.  
247 (Ed.), Oak Ridge, Tennessee, USA, 2016.

248

249 Ito, A.: Changing ecophysiological processes and carbon budget in East Asian ecosystems under  
250 near-future changes in climate: implications for long-term monitoring from a process-based  
251 model, *Journal of plant research*, 123, 577-588, 2010.

252

253 Jain, A. K. and Yang, X.: Modeling the effects of two different land cover change data sets on  
254 the carbon stocks of plants and soils in concert with CO<sub>2</sub> and climate change, *Global  
255 Biogeochem. Cycles*, 19, GB2015, 2005.

256

257 Krinner, G., Viovy, N., de Noblet-DucoudrÈ, N., OgÈe, J., Polcher, J., Friedlingstein, P., Ciais,  
258 P., Sitch, S., and Prentice, I. C.: A dynamic global vegetation model for studies of the coupled  
259 atmosphere-biosphere system, *Global Biogeochem. Cycles*, 19, GB1015, 2005.

260

261 Lei, H., Huang, M., Leung, L. R., Yang, D., Shi, X., Mao, J., Hayes, D. J., Schwalm, C. R., Wei,  
262 Y., and Liu, S.: Sensitivity of global terrestrial gross primary production to hydrologic states  
263 simulated by the Community Land Model using two runoff parameterizations, *Journal of  
264 Advances in Modeling Earth Systems*, 6, 658-679, 2014.

265

266 Liu, J., Bowman, K. W., Lee, M., Henze, D. K., Bousseres, N., Brix, H., Collatz, G. J.,  
267 Menemenlis, D., Ott, L., and Pawson, S.: Carbon monitoring system flux estimation and  
268 attribution: impact of ACOS-GOSAT X CO<sub>2</sub> sampling on the inference of terrestrial biospheric  
269 sources and sinks, *Tellus B*, 66, 2014.

270

271 Mao, J., Thornton, P. E., Shi, X., Zhao, M., and Post, W. M.: Remote Sensing Evaluation of  
272 CLM4 GPP for the Period 2000-09\*, *Journal of Climate*, 25, 5327-5342, 2012.

273

274 Olsen, S. C. and Randerson, J. T.: Differences between surface and column atmospheric CO<sub>2</sub>  
275 and implications for carbon cycle research, *Journal of Geophysical Research: Atmospheres  
276 (1984–2012)*, 109, 2004.

277  
278 Peng, C., Liu, J., Dang, Q., Apps, M. J., and Jiang, H.: TRIPLEX: a generic hybrid model for  
279 predicting forest growth and carbon and nitrogen dynamics, *Ecological Modelling*, 153, 109-130,  
280 2002.

281  
282 Ricciuto, D. M., King, A. W., Dragoni, D., and Post, W. M.: Parameter and prediction  
283 uncertainty in an optimized terrestrial carbon cycle model: Effects of constraining variables and  
284 data record length, *Journal of Geophysical Research: Biogeosciences* (2005–2012), 116, 2011.

285  
286 Schaefer, K., Collatz, G. J., Tans, P., Denning, A. S., Baker, I., Berry, J., Prihodko, L., Suits, N.,  
287 and Philpott, A.: Combined Simple Biosphere/Carnegie-Ames-Stanford Approach terrestrial  
288 carbon cycle model, *Journal of Geophysical Research*, 113, G03034, 2008.

289  
290 Schwalm, C. R., Huntzinger, D. N., Fisher, J. B., Michalak, A. M., Bowman, K., Ciais, P., Cook,  
291 R., El - Masri, B., Hayes, D., and Huang, M.: Toward “optimal” integration of terrestrial  
292 biosphere models, *Geophysical Research Letters*, 42, 4418-4428, 2015.

293  
294 Sheffield, J., Goteti, G., and Wood, E. F.: Development of a 50-year high-resolution global  
295 dataset of meteorological forcings for land surface modeling, *Journal of Climate*, 19, 3088-3111,  
296 2006.

297  
298 Sitch, S., Smith, B., Prentice, C. I., Arneeth, A., Bondeau, A., Cramer, W., Kaplan, J. O., Lucht,  
299 W., Sykes, M. T., Thonicke, K., and Venevsky, S.: Evaluation of ecosystem dynamics, plant  
300 geography and terrestrial carbon cycling in the LPJ dynamic global vegetation model, *Global  
301 Change Biology*, 9, 161-185, 2003.

302  
303 Thornton, P. E., Law, B. E., Gholz, H. L., Clark, K. L., Falge, E., Ellsworth, D. S., Goldstein, A.  
304 H., Monson, R. K., Hollinger, D., Paw U, J. C., and Sparks, J. P.: Modeling and measuring the  
305 effects of disturbance history and climate on carbon and water budgets in evergreen needleleaf  
306 forests, *Agricultural and Forest Meteorology*, 113, 185-222, 2002.

307  
308 Tian, H., Chen, G., Zhang, C., Liu, M., Sun, G., Chappelka, A., Ren, W., Xu, X., Lu, C., and Pan,  
309 S.: Century-scale responses of ecosystem carbon storage and flux to multiple environmental  
310 changes in the southern United States, *Ecosystems*, 15, 674-694, 2012.

311  
312 Weedon, G., Gomes, S., Viterbo, P., Shuttleworth, W., Blyth, E., Österle, H., Adam, J., Bellouin,  
313 N., Boucher, O., and Best, M.: Creation of the WATCH forcing data and its use to assess global  
314 and regional reference crop evaporation over land during the twentieth century, *Journal of  
315 Hydrometeorology*, 12, 823-848, 2011.

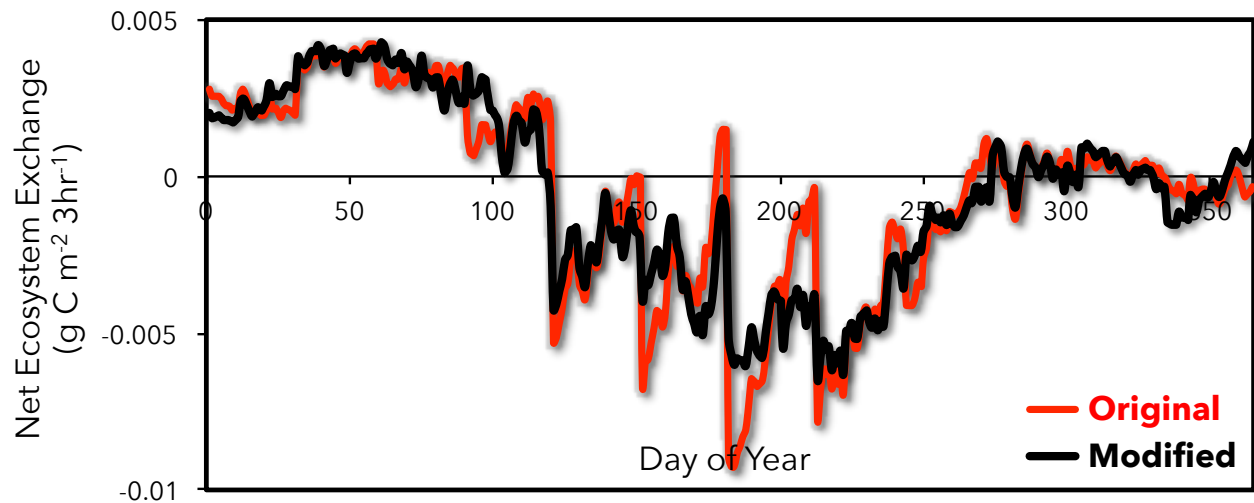
316  
317 Weedon, G. P., Balsamo, G., Bellouin, N., Gomes, S., Best, M. J., and Viterbo, P.: The WFDEI  
318 meteorological forcing data set: WATCH Forcing Data methodology applied to ERA - Interim  
319 reanalysis data, *Water Resources Research*, 50, 7505-7514, 2014.

320  
321 Wei, Y., Liu, S., Huntzinger, D., Michalak, A., Viogy, N., Post, W., Schwalm, C., Schaefer, K.,  
322 Jacobson, A., and Lu, C.: NACP MsTMIP: Global and North American Driver Data for Multi-

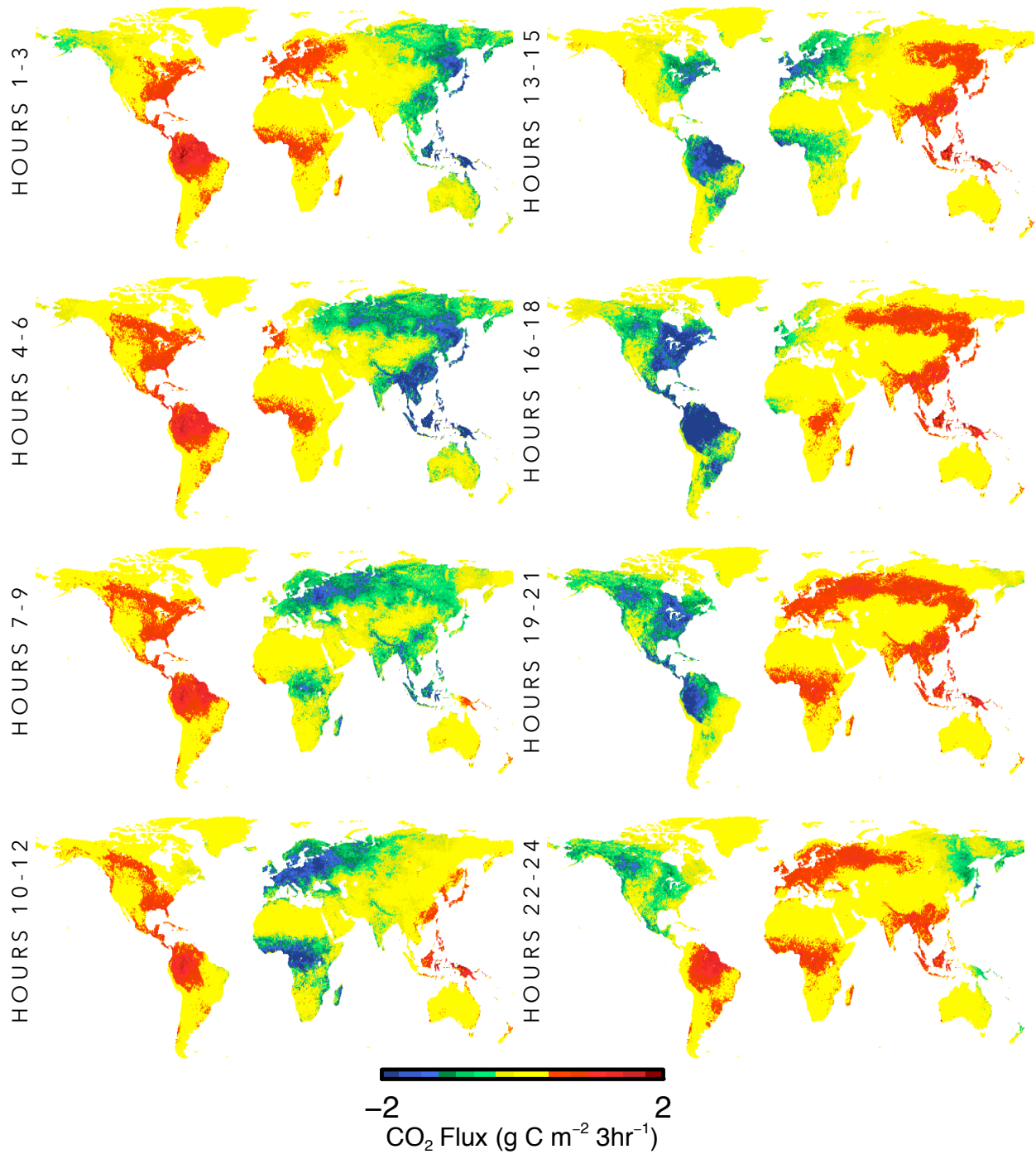
323 Model Intercomparison. Data set. Available on-line [<http://daac.ornl.gov/>] from Oak Ridge  
324 National Laboratory Distributed Active Archive Center, Oak Ridge, Tennessee, USA. 2014a.  
325  
326 Wei, Y., Liu, S., Huntzinger, D., Michalak, A., Viovy, N., Post, W., Schwalm, C., Schaefer, K.,  
327 Jacobson, A., and Lu, C.: The North American Carbon Program Multi-scale Synthesis and  
328 Terrestrial Model Intercomparison Project–Part 2: Environmental driver data, *Geoscientific*  
329 *Model Development*, 7, 2875-2893, 2014b.  
330  
331 Zeng, N., Qian, H., Roedenbeck, C., and Heimann, M.: Impact of 1998-2002 midlatitude drought  
332 and warming on terrestrial ecosystem and the global carbon cycle, *Geophys. Res. Lett.*, 32,  
333 L22709, 2005.  
334  
335

<b>Model</b>	<b>Reference</b>
BIOME_BGC	Thornton et al. (2002)
CLM	Mao et al. (2012)
CLM4VIC	Lei et al. (2014)
CLASS_CTEM	Huang et al. (2011)
DLEM	Tian et al. (2012)
GTEC	Ricciuto et al. (2011)
ISAM	Jain and Yang (2005)
LPJ-wsl	Sitch et al. (2003)
ORCHIDEE	Krinner et al. (2005)
SIB3	Baker et al. (2008)
SIBCASA	Schaefer et al. (2008)
TEM6	Hayes et al. (2011)
TRIPLEX-GHG	Peng et al. (2002)
VEGAS2.1	Zeng et al. (2005)
VISIT	Ito (2010)

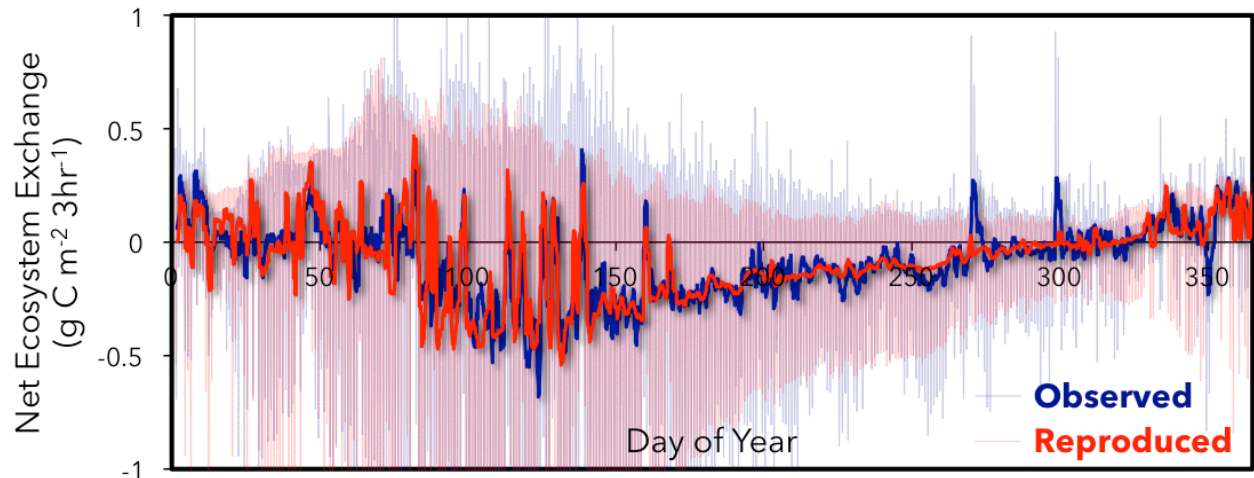
336 Table 1. Global terrestrial biosphere models from the Multi-scale Synthesis and Terrestrial  
337 Model Intercomparison Project (MsTMIP) downscaled in this activity.



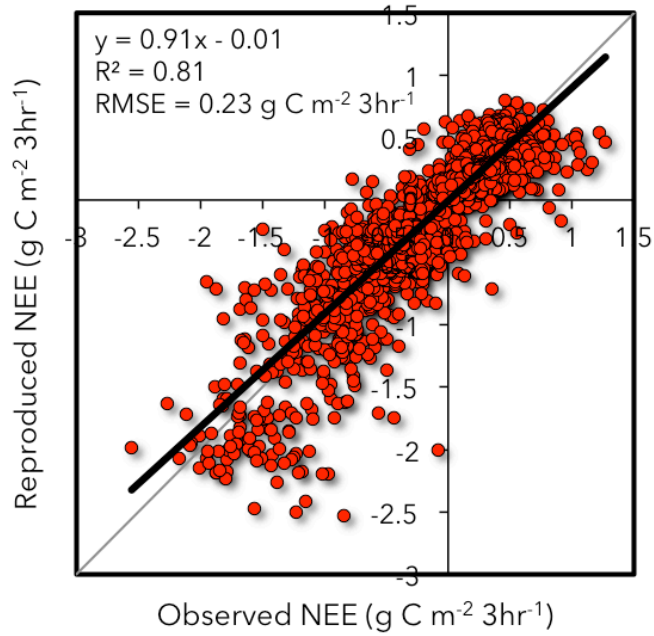
338  
 339 Figure 1. The original downscaling approach of Olsen and Randerson (2004) used monthly fixed  
 340 values, which led to a “stair-stepping” behavior between months (red). This was eliminated by  
 341 using a 30-day moving window and interpolating monthly input values to 3-hourly time steps  
 342 (black). Example shown for LPJ model global mean year 2005.



343 Figure 2. Vegetation productivity (e.g., blues/greens) follows the course of the sun for a single  
 344 day of net ecosystem exchange (NEE or net CO<sub>2</sub> flux; g C m<sup>-2</sup> 3hr<sup>-1</sup>) for each 3-hourly period.  
 345 Shown here, for example, is July 1, 2007 for the weighted ensemble mean product.



346  
 347 Figure 3. The observed net ecosystem exchange (NEE) (blue) and reproduced NEE (red) shown  
 348 at the 3-hourly time step with daily moving window overlaid for a single year from the Tonzi  
 349 Ranch AmeriFlux/FLUXNET site (Baldocchi and Ma, 2013).



350  
351 Figure 4. Observed versus reproduced net ecosystem exchange (NEE) at the 3-hourly time step  
352 for a single year at the Tonzi Ranch AmeriFlux/FLUXNET site (Baldocchi and Ma, 2013).